ARL-TR-10171 ● SEP 2025

Variations of Thermal Conductivity with Porous Silicon Layer Thickness

by Matthew H. Ervin and Aaron J. Henson

NOTICES

Disclaimers

The findings in this report are not to be construed as an official Department of the Army position unless so designated by other authorized documents.

Citation of manufacturer's or trade names does not constitute an official endorsement or approval of the use thereof.

Destroy this report when it is no longer needed. Do not return it to the originator.

ARL-TR-10171 ● SEP 2025

Variations of Thermal Conductivity with Porous Silicon Layer Thickness

Matthew H. Ervin and Aaron J. Henson
DEVCOM Army Research Laboratory

REPORT DOCUMENTATION PAGE

1. REPORT DATE	2. REPORT TYPE	3. DATES COVERED	
		START DATE	END DATE
September 2025	Technical Report	01-01-2023	12-31-2023

4. TITLE AND SUBTITLE
Variations of Thermal Conductivity with Porous Silicon Layer Thickness

5a. CONTRACT NUMBER	5b. GRANT NUMBER	5c. PROGRAM ELEMENT NUMBER
5d. PROJECT NUMBER	**5e. TASK NUMBER**	**5f. WORK UNIT NUMBER**

6. AUTHOR(S)
Matthew H. Ervin and Aaron J. Henson

7. PERFORMING ORGANIZATION NAME(S) AND ADDRESS(ES)
DEVCOM Army Research Laboratory
ATTN: FCDD-RLA-LB
Aberdeen Proving Ground, MD 21005

8. PERFORMING ORGANIZATION REPORT NUMBER
ARL-TR-10171

9. SPONSORING/MONITORING AGENCY NAME(S) AND ADDRESS(ES)	10. SPONSOR/MONITOR'S ACRONYM(S)	11. SPONSOR/MONITOR'S REPORT NUMBER(S)

12. DISTRIBUTION/AVAILABILITY STATEMENT
DISTRIBUTION STATEMENT A. Approved for public release: distribution unlimited.

13. SUPPLEMENTARY NOTES

14. ABSTRACT
Porous silicon has many useful properties, which differ from those of bulk silicon. For instance, porous silicon has significantly lower thermal conductivity. This can be advantageous for some applications, but a problem for others. Therefore, understanding the thermal conductivity of porous silicon layers is important. We have discovered that the thicker the porous silicon layer, the lower its thermal conductivity. This may be due to an increase in its porosity due to an additional chemical etching mechanism or to increased phonon–phonon scattering as the temperature increases with the thickness of the thermally insulating porous silicon layer.

15. SUBJECT TERMS
Electromagnetic Spectrum Sciences, porous silicon, thermal conductivity, thermal diffusivity, porous silicon etch

16. SECURITY CLASSIFICATION OF:			17. LIMITATION OF ABSTRACT	18. NUMBER OF PAGES
a. REPORT	b. ABSTRACT	C. THIS PAGE		
UNCLASSIFIED	UNCLASSIFIED	UNCLASSIFIED	UU	18

19a. NAME OF RESPONSIBLE PERSON	19b. PHONE NUMBER *(Include area code)*
Matthew H. Ervin	(520) 691-5542

STANDARD FORM 298 (REV. 5/2020)
Prescribed by ANSI Std. Z39.18

Contents

List of Figures

1. Introduction

Porous silicon (pSi)—formed by the electrochemical etching of silicon (Si)—is a technologically useful material with many interesting characteristics. It can be formed with nano- to macro-pore sizes and with low to high porosities yielding a wide range of properties. Porous silicon is used for its light-absorbing properties in solar cells and photodetectors, light-emitting properties in optoelectronics, large specific surface area in chemical sensors, biodegradability in drug delivery, and low thermal conductivity in thermoelectric generators/coolers, among others (Kurbanova et al. 2004; Erfantalab et al. 2022). Energetic applications use its high surface area and small crystallite size to enable rapid chemical reactions with oxidizers loaded into the pores (Piekiel et al. 2015). This report focuses on pSi's low thermal conductivity, which is beneficial for some applications and deleterious for others. When combined with traditional Si semiconductor devices, pSi can interfere with the removal of waste heat causing degraded device performance or device failure due to overheating and metal electromigration (Cahill et al. 2003). Conversely, low thermal conductivity is beneficial to thermoelectric generators/coolers and IR sensors.

The reduced thermal conductivity of pSi, as compared with bulk Si, is caused by two factors.

1) The pSi is a mixture of Si (which conducts heat well) and void (i.e., air—which conducts heat poorly). Thus, as the porosity increases the thermal conductivity decreases (Gesele et al. 1997; Haseeb 2023; Isaiev et al. 2023).
2) As the pore wall dimensions decrease (i.e., until they are smaller than the phonon mean free path in bulk Si (i.e., ~40 nm in Si [Chen 1996; Gesele et al. 1997]), they limit the phonon mean free path. The phonon mean free paths are reduced as phonons are scattered off pore wall interfaces; thus, slowing the phonon transport of heat (De Boor et al. 2011; Haseeb 2023; Isaiev et al. 2023).

The passivation of the pore walls can also have a significant effect on thermal conductivity. However, hydrogen passivation of pSi, which results from electrochemical etching with hydrofluoric-acid–based etchants, does not significantly affect the thermal conductivity (Fedorov and Teplinskaia 2022).

In semiconductors, electron conduction of heat is much lower than phonon conduction, so that phonon conduction is the dominant mechanism (Weißmantel and Hamann 1980). Even if electron conduction of heat were significant, the situation would be much the same, as pSi has electrical conductivity up to 7 orders

of magnitude lower than the underlying wafer (Haseeb 2023). Interestingly, the specific heat capacity increases monotonically with porosity (Erfantalab et al. 2022; Fedorov and Teplinskaia 2022) when using p-type Si. This increase in heat capacity has been attributed to a shift of the phonon density of states to lower, more accessible energies (Fedorov and Teplinskaia 2022). It has been reported that the specific heat capacity goes down with porosity for n-type Si (Hernandez-Wong et al. 2025).

Lang et al. (1994) first reported that pSi has thermal conductivity much lower than bulk Si. Precise thermal conductivity is a function of porosity, pore size, pore density, pore geometry, and Si doping; however, it is typically reported to be 2+ orders of magnitude less than bulk Si (Gesele et al. 1997; Haseeb 2023). Even with a low porosity of 5%, the thermal conductivity can be reduced by 90% if the pores are small, which yields a large total internal surface area (Verdier et al. 2017). This is especially the case when the pore structure is very disordered, as with highly p-doped Si (Verdier et al. 2017). The anisotripic nature of the electrochemically etched pores, which are typically aligned primarily perpendicular to the film surface, results in thermal conductivities that are different when parallel to and perpendicular to the surface of the pSi film.

The thermal properties of pSi are temperature dependent. The thermal conductivity is reported by Gesele et al. (1997) to increase linearly with temperature (35–320 K) for p-type and 64%–89% pSi. This was explained as being due to increasing heat capacity with temperature as more phonon states are energetically available (Gesele et al. 1997). Gesele et al. (1997) also explain that p+ (0.01 Ω cm) pSi has a four times higher thermal conductivity than that formed on lower doped (0.2 Ω cm) p-type Si due to the different pore structures. Interestingly, the thermal conductivity and heat capacity were reported to go down for n-type pSi (Hernandez-Wong et al. 2025). This is similar to bulk Si, which has a decreasing thermal conductivity with increasing temperature (Gesele et al. 1997).

Given its importance, it is no surprise there are many methods for measuring the thermal conductivity of pSi films (Erfantalab et al. 2022). There are noncontact methods where the material has energy injected via illumination with a resulting thermal effect measured: photoacoustic spectroscopy, laser pump–probe, lock-in thermography, and scanning micro-Raman spectroscopy. And, there are contact methods where a heater is deposited on the material or a heat source contacts the material under test with a measurement of the sample temperature: the 3 ω method, transient thermo-reflectance, or scanning thermal microscopy. In this work, thermal diffusivities were measured by a commercial laboratory (Dynalene Inc.) using a noncontact laser flash method.

Here, we report measurements of the thermal conductivity of pSi films of differing thicknesses. The thermal conductivity values (k) were calculated using measured thermal diffusivity (α), density (ρ), and specific heat (C_p) values:

$$k = \alpha * \rho * C_p \quad (1)$$

Surprisingly, the thermal conductivity of pSi films goes down with increasing layer thickness. This leaves the possibility of tuning the thermal conductivity of a pSi layer to the needs of the device.

2. Experimental Procedure

2.1 Thermal Diffusivity Measurements

The thermal diffusivity measurements have been reported in detail previously (Ervin 2023) and are summarized here. Samples were made for thermal diffusivity measurements using 6–9 Ω cm p-type (100) double-sided polished Si. Selective-area, gold electrodes were deposited onto the backside of Si die to produce more-uniform pSi film thicknesses (Piekiel et al. 2019). The pSi films were electrochemically etched with a 3D-printed etch well using a no. 14 O-ring to define the area to be etched. A 3:1 concentrated hydrofluoric acid to absolute ethanol etch solution and a platinum wire counter electrode were placed into the well to complete the etch cell. The positive terminal of a power supply was attached to the gold backside electrode and the negative terminal was attached to the platinum counter-electrode. The etch depth is determined by the etch current and time. After the etch, the gold electrode is removed with a potassium iodide solution, being careful not to expose the pSi. An LPKF U4 laser mill was then used to cut 12.6-mm-diameter pSi/Si samples out of the die. This size matches the 0.5-inch sample holder of the Netzsch model LFA 447 Nanoflash instrument used. The pSi produced is too fragile to be used as standalone films, which is why the test samples consisted of pSi films on Si substrates mounted onto aluminum disks with Bergquist TGF4000—a high-conductivity, silicone-based thermal gap filler. This sample structure represents the actual application more faithfully than a freestanding film because the interfaces between the pSi and Si substrate and the heat sink have important effects on the heat sinking ability of the whole device. The sample surfaces were coated with thin graphite films containing known surface emissivities for the measurements.

2.2 Density Measurements

Duplicate samples were etched for making the film thickness and density measurements. The pSi film densities were measured using a Hitachi model S-4500 scanning electron microscope to measure cross-sectional film thicknesses, and a Mettler Toledo XP26 balance to measure the mass of Si in the pSi films. The differences in mass of the unetched die and the die after the pSi has been removed with a 1 mol/L sodium hydroxide solution represents the amount of Si in the pSi layers. The volume of the films is calculated by multiplying the sample area times the average film thickness measured across a cross section of the film. The thickness averages were weighted by the area represented at each measured radius. This weighted average is important because the pSi films were thicker in the sample centers.

2.3 Specific Heat Measurements

The specific heat of pSi was determined using a Perkin Elmer differential scanning calorimeter (model DSC 8500). The samples for DSC were prepared by etching a monolithic layer of pSi into a Si substrate and subsequently electropolishing through a current pulse to lift off the pSi without damaging the pores. The flakes from lift-off were then washed and dried and used for DSC measurements. To conduct the test, a sample is loaded in chamber 1, while an empty pan is loaded in chamber 2. The DSC measures the amount of energy required to raise the temperature at a specific rate, which then subtracts the energy required for the empty pan in chamber 2. The DSC measurements were taken across 20 °C intervals, centered on the temperature of interest. Each measurement is calibrated with a sapphire control, as sapphire has a well-documented and consistent specific heat. Each DSC measurement was taken across a 20 °C range at 20 °C/min ramp rate with each test containing two cycles. The specific heat was found at multiple temperatures, with the final equation for the sample's specific heat shown here:

$$C_{sample} = \frac{\Delta y_{sample}}{\Delta y_{sapphire}} \cdot \frac{m_{sapphire}}{m_{sample}} \cdot C_{sapphire} \quad (2)$$

3. Results and Discussion

3.1 Specific Heat Results

The resulting specific heat measurements at different temperatures are shown in Figure 1. Our results show that the heat capacity goes up with temperature. This agrees with Gesele et al.'s (1997) conclusions that heat capacity increases with temperature as more phonon states are energetically available, which is unsurprising since we are using similar pSi material.

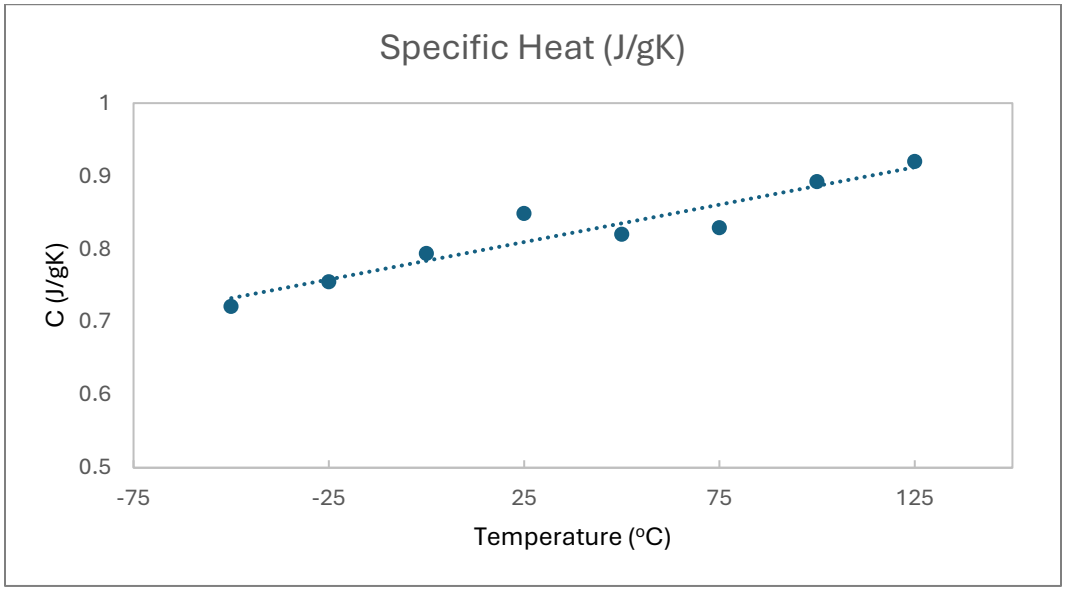

Figure 1. Specific heat of pSi as a function of temperature.

Specific heat values reported in literature for pSi range from 0.8 to 2.1 J/gK for porosities ranging from 45% to 77% (Erfantalab et al. 2022). The specific heat is heavily dependent on the percent porosity of the material with higher porosities exhibiting lower specific heat values. The values measured in this study confirm a very highly porous material as we are on the low end of the range of values reported in literature.

3.2 Thermal Conductivity Results

Once the specific heat, thermal diffusivity, and density of the pSi and pSi/Si bilayer samples were measured, the following calculations were performed to isolate the properties of the pSi alone.

Assuming steady-state heat transfer, total thermal resistance equals

$$R_{total} = \Sigma R_{t_j} \tag{3}$$

$$R_t = \frac{w}{kA} \tag{4}$$

where w = thickness of pSi layer, k = thermal conductivity, and A = area. For a two-layer steady-state system, this becomes

$$R_{total} = \frac{w_{total}}{k_{total} * A_{total}} = \frac{w_1}{k_1 * A_1} + \frac{w_2}{k_2 * A_2} \tag{5}$$

For the pSi/Si bilayer samples, k_{total} can be calculated using the following:

$$k_{total} = \alpha_{total} * C_{p_{total}} * \rho_{total} \tag{6}$$

where α_{total} was the thermal diffusivity measured of the bilayer of pSi and Si, ρ_{total} is the density of the combined bilayer material, which can easily be calculated knowing the mass and volume of each material. The $C_{p_{total}}$ is the specific heat of the combined material, which can be calculated if you know the specific heats of the two individual materials using a weighted average as follows:

$$mc = \Sigma m_i c_i \tag{7}$$

where m = mass and c = specific heat. For our system this is easily calculated by knowing the total mass of pSi and Si and their respective specific heats. Assuming the system is in thermal equilibrium, we calculate the following:

$$c_{total} = \frac{c_{pSi} m_{pSi} + c_{Si} m_{Si}}{m_{total}} \tag{8}$$

Once we have the c_{total} we can calculate the k_{total}, which we can then put back into Equation 3 and solve for pSi and Si.

$$k_{pSi} = \frac{w_{pSi}}{(A_{pSi})\left(\left(\frac{w_{total}}{k_{total} A_{total}}\right) - \left(\frac{w_{Si}}{(k_{Si} A_{Si})}\right)\right)} \tag{9}$$

Figure 2 shows the thermal conductivity of pSi as a function of layer thickness obtained from the preceding calculations.

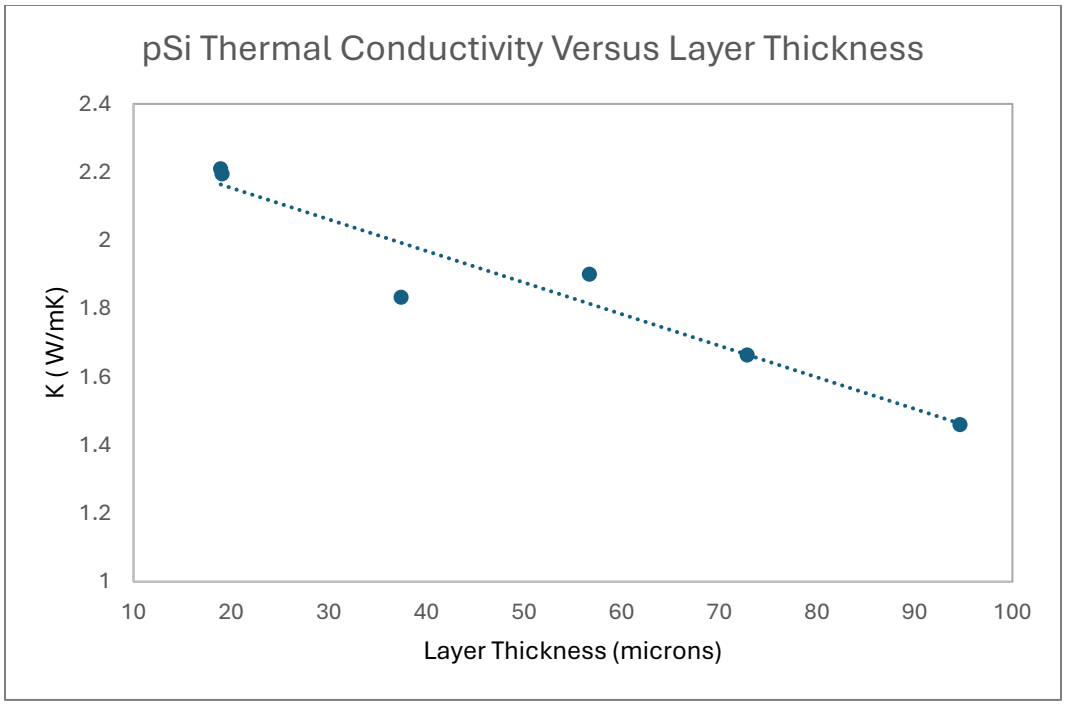

Figure 2. Thermal conductivity of pSi as a function of layer thickness.

Generally, thermal conductivity is a constant property of bulk solids. Thermal conductivity of porous materials, however, is significantly more complex compared with bulk solids. This is especially true in the present case as the porosity may change with film thickness. This may be due to two reasons. First, as the etch depth gets deeper it is harder for the etchant hydrofluoric acid to diffuse to the pore tip to continue the etching. This can cause a concentration gradient in the pore that effectively changes the etchant concentration at the pore tip. Etchant concentration has significant effects on the etched porosity/pore size. Second, while the electrochemical etching has the largest effects on the pore size/density in the pSi layer, there is also a slower chemical etch that continues after the pores are formed. This etch enlarges the pores and thins the pore walls, increasing the porosity of the pSi. In thicker films, the near surface material becomes more porous, as it is subjected to this chemical etch for longer than the deeper, more freshly etched material. This effect would be more pronounced for longer etch times, and it would result in a higher average porosity for thicker films. As a result, thicker films would have lower thermal conductivities.

Another potential mechanism for decreasing thermal conductivity with thicker pSi layers is an Anderson localization mechanism (Ferrando-Villalba et al. 2018). In simple terms, a thicker pSi layer presents a larger barrier to thermal energy transport, trapping more heat. This increases the temperature near the Si/pSi interface so that there are more phonons and therefore more phonon–phonon

scattering, which impedes the heat transfer further. This results in lower measured thermal conductivity of the overall pSi layer.

4. Conclusions

The thermal conductivity of pSi has been measured and found to be similar to that reported previously in the literature. However, it was discovered that the thermal conductivity goes down with film thickness. This could be due to increasing porosity from slow chemical etching, which takes place after the pores are electrochemically formed. This effect could also be caused by increased phonon–phonon scattering due to increased heat transport near the Si/pSi interface. Decreasing thermal conductivity with increasing pSi layer thickness may be an important consideration for applications requiring a specific thermal conductivity; however, for most applications it is sufficient to know that the thermal conductivity of the pSi is orders of magnitude lower than that of the bulk Si.

5. References

Cahill D et al. Nanoscale thermal transport. J App Phys. 2003;93:793–818. https://doi.org/10.1063/1.1524305

Chen G. Nonlocal and nonequilibrium heat conduction in the vicinity of nanoparticles. ASME J Heat Transf, 1996;118(3):539–545.

De Boor J et al. Temperature and structure size dependence of the thermal conductivity of porous silicon. EPL. 2011;96:16001. https://doi.org/10.1209/0295-5075/96/16001

Erfantalab S Parish G, Keating A. Determination of thermal conductivity, thermal diffusivity and specific heat capacity of porous silicon thin films using the 3ω method. Int J Heat Mass Transf. 2022; 184. https://doi.org/10.1016/ j.ijheatmasstransfer.2021.122346

Ervin M. Porous silicon thermal diffusivity. DEVCOM Army Research Laboratory (US); 2023 Aug. Report.: ARL-TR-9758.

Fedorov A, Teplinskaia A. Thermal properties of porous silicon nanomaterials. Materials. 2022;15:8678. https://doi.org/10.3390/ma15238678

Ferrando-Villalba P et al. Impact of pore anisotropy on the thermal conductivity of porous Si nanowires. Sci Rep. 2018;8(1):12796. https://doi.org/10.1038/s41598-018-30223-0

Gesele G, Linsmeier J, Drach V, Fricke J, Arens-Fischer R. Temperature-dependent thermal conductivity of porous silicon. J Phys D Appl Phys. 1997;30:2911–2916.

Haseeb H. Charge and heat transport across interfaces in nanostructured porous silicon [dissertation]. Institute for Physics and Astronomy University of Potsdam; 2023.

Hernandez-Wong J et al. Analytical models for the thermal properties of n-type porous silicon layer: dependence of porosity. J Appl Phys. 2025;137:085103. https://doi.org/10.1063/5.0250168

Isaiev M, Mankovska Y, Kuryliuk V, Lacroix D. Thermal transport properties of nanoporous silicon with significant specific surface area. Appl Phys Lett. 2023;122:172201. https://doi.org/10.1063/5.0148434

Kurbanova B et al. Multiscale phonon thermal transport in nano-porous silicon. Appl Phys Lett. 2004;124:252202. https://doi.org/10.1063/5.0205455

Lang W, Drost A, Steiner P, Sandmaier H. The thermal conductivity of porous silicon. MRS Online Proc Lib Arch. 1994;358.

Piekiel N et al. Combustion and material characterization of highly tunable on-chip energetic porous silicon. Propellants Explos Pyrotech. 2015;40:16–26. https://doi.org/10.1002/prep.201400140

Piekiel N et al. Improved galvanic porous silicon fabrication using patterned electrodes. Sens Actuators A Phys. 2019;286:195–201.

Verdier M, Termentzidis K, Lacroix D. Modeling thermal transport in nano-porous semiconductors. In: Bettotti P, editor. Submicron Porous Materials. Springer; 2017. https://doi.org/10.1007/978-3-319-53035-2_9

Weißmantel C, Hamann C. Grundlagen der Festkörperphysik. Springer; 1980. p. 419.

List of Symbols, Abbreviations, and Acronyms

3D	three-dimensional
DSC	differential scanning calorimeter
IR	infrared
pSi	porous silicon
Si	silicon

1 (PDF)	DEFENSE TECHNICAL INFORMATION CTR DTIC OCA
1 (PDF)	DEVCOM ARL FCDD RLB CI TECH LIB